Title

Isolation, Structure Elucidation, and Iron-Binding Properties of Lystabactins, Siderophores Isolated from a Marine Pseudoalteromonas sp.

Journal

Journal of Natural Products, 76(4)

ISSN

0163-3864 1520-6025

Authors

Zane, Hannah K

Butler, Alison

Publication Date

2013-04-26

DOI

10.1021/np3008655

Isolation, Structure Elucidation and Iron Binding Properties of Lystabactins, Siderophores Isolated from a Marine *Pseudoalteromonas sp.*

Hannah K. Zane and Alison Butler[*]

Department of Chemistry and Biochemistry, University of California, Santa Barbara,

California 93106-9510

RECEIVED DATE (to be automatically inserted)

* To whom correspondence should be addressed. Tel: 805-893-8178. Fax: 805-893-4120. Email: butler@chem.ucsb.edu

ABSTRACT:

The marine bacterium *Pseudoalteromonas* sp. S2B, isolated from the Gulf of Mexico after the Deepwater Horizon oil spill, was found to produce lystabactins A, B and C (**1**-**3**), three new siderophores. The structures were elucidated through mass spectrometry, amino acid analysis and NMR. The lystabactins are comprised of serine (Ser), asparagine (Asn), two formylated/hydroxylated ornithines (*FOH*Orn), dihydroxy benzoic acid (Dhb) and a very unusual nonproteinogenic amino acid, 4,8-diamino, 3-hydroxy octanoic acid (LySta). The iron binding properties of the compounds were investigated through a spectrophotometric competition.

Iron is essential for the growth of nearly all bacteria. However, the limited solubility of iron(III) in aqueous aerobic environments means iron is not readily available for many microbes. For marine bacteria, the challenge in obtaining enough iron for growth is exacerbated because of the low concentration of iron throughout much of the world's oceans.[1-5] Most bacteria are thought to require micromolar concentrations of iron for growth, while the sea water iron concentration is simultaneously less than micromolar.[1-5] Many microbes have evolved multiple strategies to obtain iron from their surroundings, one of which is the production of siderophores.[6, 7] Siderophores are low molecular weight iron(III) chelators which solubilize and transport iron(III) into the cell.[6, 7]

The marine environment is subject to contamination by organic pollutants from a variety of sources.[8, 9] Crude oil is a substantial organic pollutant in marine environments.[8, 9] Fortunately, a significant portion of oil in the marine environment is eliminated by the hydrocarbon-degrading activities of different organisms, including bacteria.[8, 9] The rate of microbial biodegradation is influenced by the availability of nutrients; specifically nitrogen, phosphorus, and iron.[10, 11] Siderophores may play a role in biodegradation by facilitating acquisition of iron, a limiting nutrient in the ocean, as well as in other environments.[12, 13]

While adding iron to a hydrocarbon-degrading bacterial culture can stimulate the biodegradation rate,[14, 15] the mechanisms of iron acquisition by these microbes have not been well studied. Siderophore production by the oil-degrading *Marinobacter hydrocarbonoclasticus* was investigated, and it was found to produce petrobactin, a bis-catecholate, α-hydroxy siderophore.[16, 17] As a result of the α–hydroxy carboxylate group, the Fe(III)-complex of petrobactin is photoreactive in natural sunlight.[16, 17] Recently, a *Vibrio* species isolated from the

These Gulf of Mexico after the BP oil spill was found to produce the suite of amphiphilic ochrobactins-OH siderophores, which are also photoreactive when complexed to Fe(III).[18]

We report the structural characterization and iron(III) binding properties of lystabactin A, B and C (**1**-**3**), three related siderophores, produced by *Pseudoalteromonas sp*. *S2B* isolated from the Gulf of Mexico after the 2010 Deepwater Horizon oil spill.

1

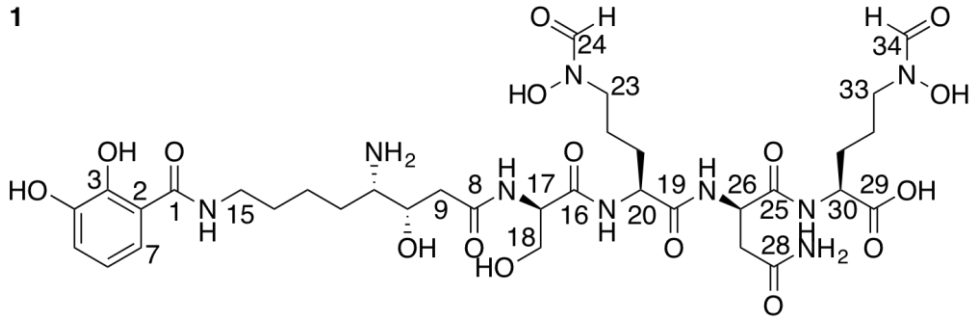

2

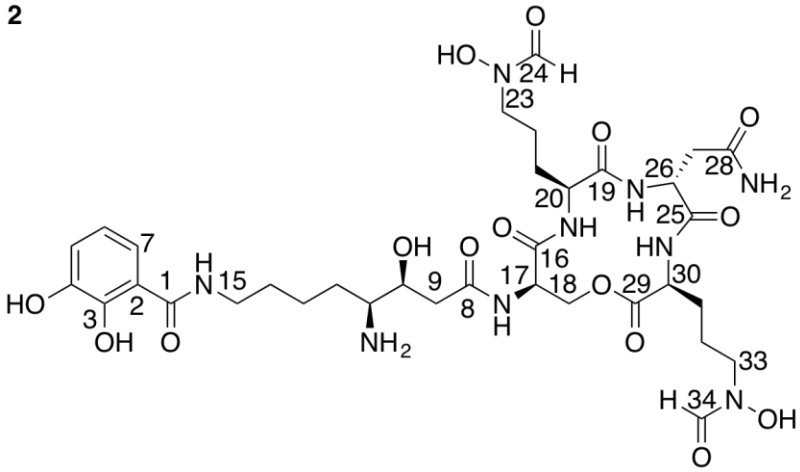

3

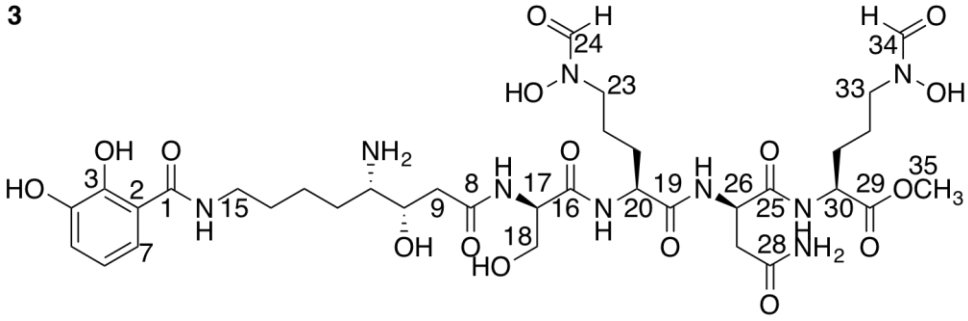

RESULTS AND DISCUSSION

The bacterial isolate was obtained from the oil-contaminated surface water of the Gulf of Mexico following the Deepwater Horizon oil spill in April 2010. A 16S rRNA sequence analysis revealed that the isolate belongs to the genus *Pseudoalteromonas* and we designate this strain as *Pseudoalteromonas sp.* S2B. To screen for hydrocarbon degrading capabilities, *Pseudoalteromonas sp*. *S2B* was grown in a synthetic seawater medium supplemented with crude oil as the sole carbon source.[19] Bacterial growth was determined by measuring the optical density of the culture at 600 nm. *Pseudoalteromonas sp. S2B* was able to grow in an oil-supplemented medium, reaching stationary phase after around four days (Figure S1), demonstrating that the strain is able to use crude oil as the sole source of carbon.

For siderophore isolation, *Pseudoalteromonas sp. S2B* was grown in a low iron artificial seawater medium. The siderophores were isolated from the supernatant using solid-phase extraction followed by RP-HPLC. Siderophores were identified using the chrome azurol S (CAS) assay for iron(III)-binding activity. Three peaks in the HPLC chromatogram gave a positive CAS response, consistent with the presence of apo-siderophores (Figure 1).[20]

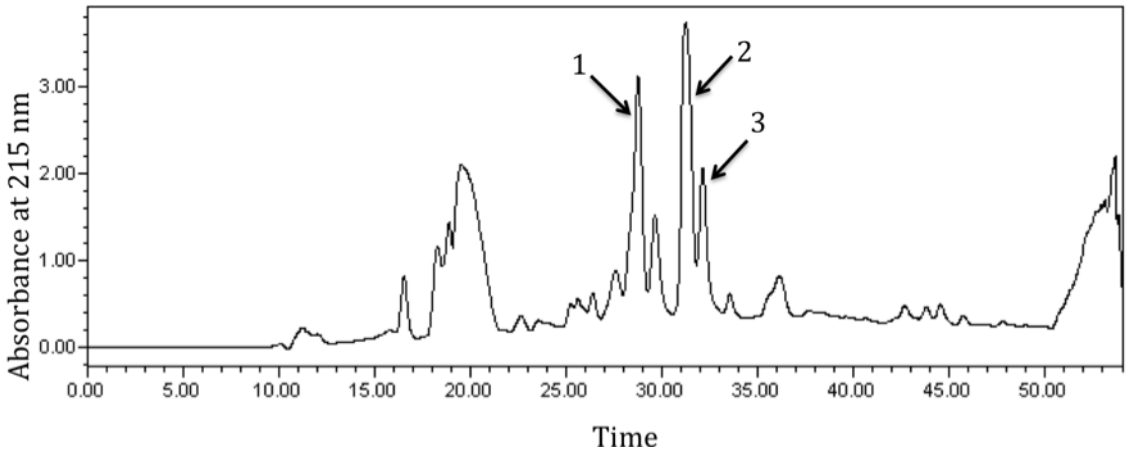

Figure 1. HPLC chromatogram illustrating three peaks that bound Fe(III) in the Fe(III)-CAS assay.

High-resolution electrospray ionization mass spectrometry (HRESIMS) established the mass of the molecular ion $[M + Na]^+$ of lystabactin A (**1**) as *m/z* 866.3484, corresponding to a molecular formula of $C_{34}H_{53}N_9O_{16}Na$. Analysis of the fragmentation pattern observed in the ESIMS/MS spectrum of **1** suggests a peptide composed of dihydroxy benzoic acid (Dhb), 4,8-diamino, 3-hydroxy octanoic acid (LySta),[21] serine (Ser), asparagine (Asn) and two formylated/hydroxylated ornithines (*FOH*Orn). Relevant fragment ions are circled in the ESIMS/MS in Figure 2 and presented in Table 1.

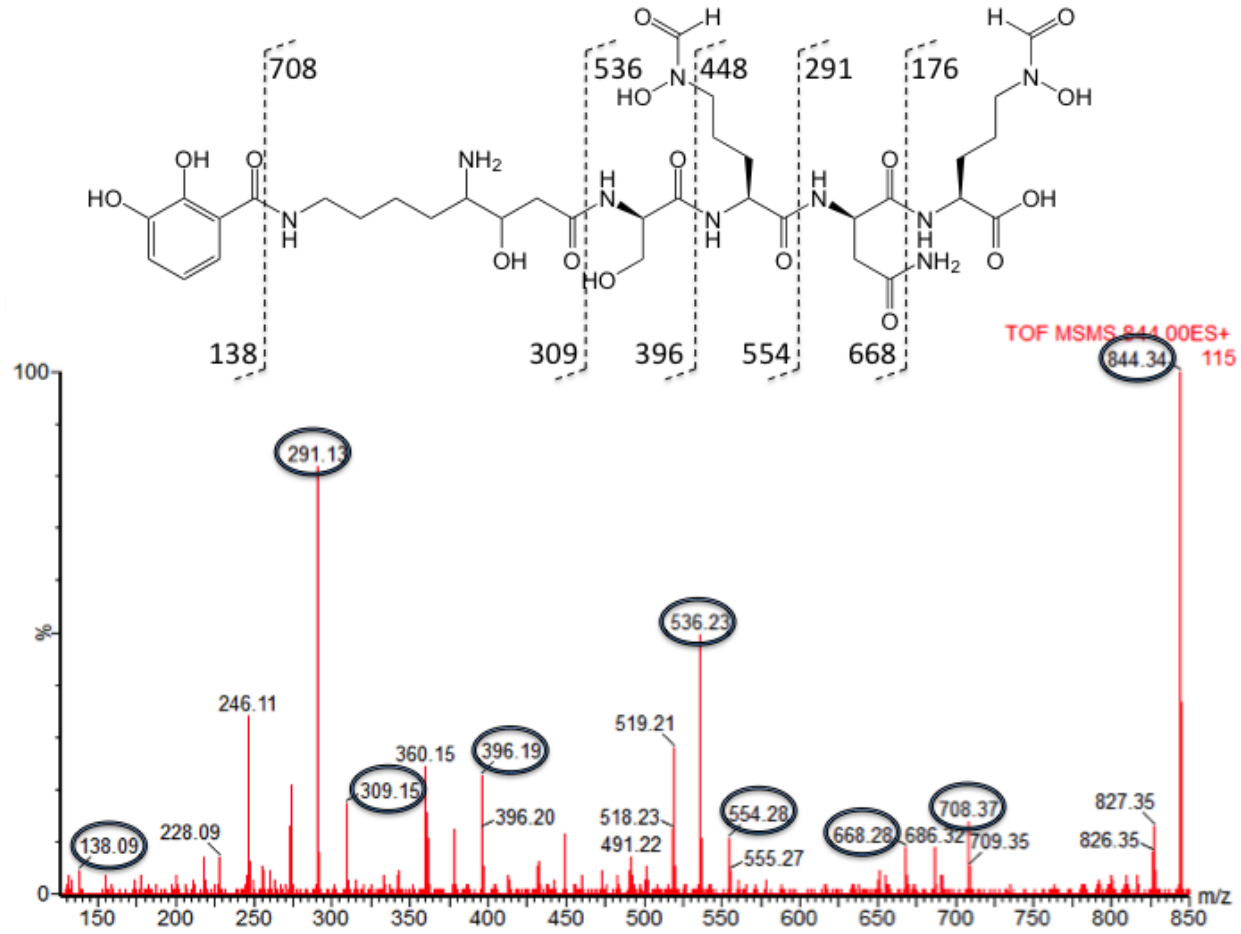

Figure 2. ESIMS/MS of Lystabactin A (**1**).

Table 1. Mass Fragments of Lystabactin A (**1**)

$[M+H]^+$	Fragment
844.44	Lystabactin A (parent ion)
668.28	Loss of N-formyl-hydroxyornithine
554.28	Loss of asparagine
396.10	Loss of N-formyl-hydroxyornithine
309.15	Loss of serine
138.09	Loss of LySta[21]

^{1}H, TOCSY and COSY NMR experiments confirmed the amino acid content of the peptide deduced from the fragment ions in the ESIMS/MS. Six individual spin systems were identified in the NMR spectra corresponding to the five amino acids in addition to 2,3-Dhb (Table 2, Figure 3). A significant feature of the spectra is the diagnostic splitting pattern of the aromatic resonances of Dhb in the ^{1}H NMR spectrum which confirm the ortho- and meta-hydroxy positions on the benzoic acid. Also of note are the two ^{1}H signals of the N-formyl group that are distinguishable due to a cis/trans-equiilibrium, in agreement with previous reports.[22] Vicinal ^{1}H-^{1}H and long range ^{13}C-^{1}H couplings were crucial in the identification of the unusual LySta residue (Table 2, Figure 3).

Table 2. NMR Data for Lystabactin A (**1**) (600 MHz) in CD_3OD

	Position	δC, type	δH (*J* in Hz)	COSY	HMBC
DHB	1	171.4, C			
	2	116.9, C			
	3	150.1, C			
	4	147.3, C			
	5	119.35, CH	6.84, d (8.0)	6	2, 3, 4, 6, 7
	6	119.37, CH	6.63, t (8.0)	5, 7	1, 2, 3, 4, 5, 7
	7	118.4, CH	7.12, d (8.0)	6	1, 2, 3, 4, 5, 6

LySta	8	173.5, C			
	9	41.1, CH_2	2.49, m	10	8, 10, 11
	10	68.4, CH	3.99, m	9, 11	8, 9, 11, 12
	11	56.7, CH	3.12, m	10, 12	9, 10, 12, 13, 14
	12	30.5, CH_2	1.73, m	11, 13	10, 11, 13, 14
	13	23.9, CH_2	1.59, m	12, 14	11, 12, 14
	14	23.5, CH_2	1. 43, m	13, 15	11, 12, 13, 15
	15	39.7, CH_2	3.33, m	14	1, 12, 13, 14
Ser	16	172.6, C			
	17	57.0, CH	4.32, m	18	8, 16, 18
	18	62.5, CH_2	3.74	17	16,17
FOHOrn	19	173.3, C			
	20	53.23	4.33 [1H]	21	16,19, 21, 22
	21	28.8	1.77	20, 22	20, 22, 23
	22	28.99, CH_2	1.63	21, 23	20, 21, 23
		50.4, CH_2 (cis)	3.43(cis)		
	23	47.0, CH_2 (trans)	3.48 (trans)	24	21, 22, 24
		159.7, CH (cis)	7.85 (cis)		
	24	163.2, CH (trans)	8.20 (trans)	23	23
Asn	25	172.1, C			
	26	51.6, CH	4.68	27	19, 25, 26, 27, 28
	27	37.6, CH_2	2.73, m; 2.54, m	26	25, 26, 28
FOHOrn	28	175.3, C			
	29	171.4, C			
	30	54.8, CH	4.18, m	31	25, 29, 31, 32
	31	28.8, CH_2	1.69, m	30, 32	30, 32, 33
	32	29.0, CH_2	1.50, m	31, 33	30, 31, 33
	33	50.4, CH_2 (cis)	3.43(cis), m		
		47.0, CH_2 (trans)	3.48 (trans), m	32, 34	31, 32, 34
	34	159.7, CH (cis)	7.86 (cis), s		
		163.2, CH (trans)	8.18 (trans), s	33	33

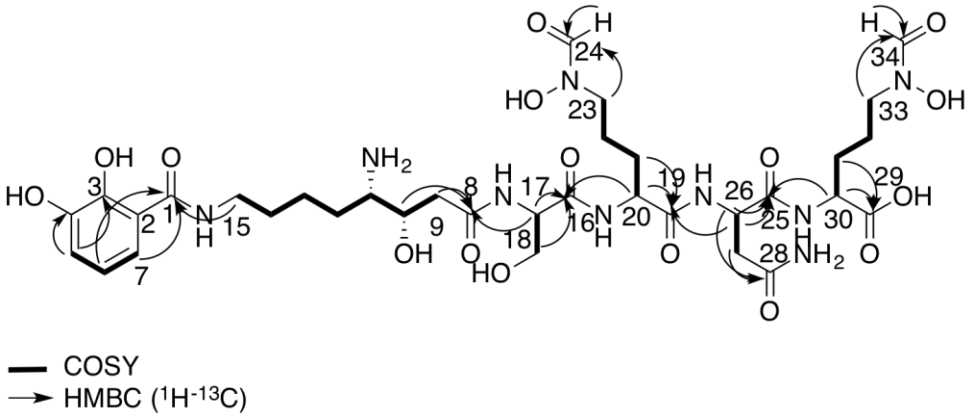

Figure 3. Lystabactin A (**1**) depicted with ^{1}H-^{1}H correlations (bold lines) and key HMBC (H→C) correlations of **1**.

The determination of the amino acid configuration of **1** was conducted by derivatization with FDAA,[23] following reductive hydrolysis using 55% HI.[24] The derivitized sample was then subjected to HPLC. The retention times of the peaks were then compared with derivitized amino acid standards revealing the presence of D-Ser, D-Asn, L-*FOH*Orn and (3S,4S)-LySta.

HRESIMS established the mass of the moleclular ion $[M + H]^+$ of lystabactin B (**2)** as *m/z* 826.3564, corresponding to a molecular formula of $C_{34}H_{52}N_9O_{15}$. The mass of this peak is 18 mass units less than lystabactin A (**1)**, suggesting a possible dehydration process. Analysis of the NMR spectra of lystabactin B (**2)** showed many similarities to **1**, however, a key difference is the downfield shift of the serine β-hydrogens to 4.38 and 4.19 ppm (compared to 3.74 ppm in **1**), consistent with the presence of a seryl ester (Table S2). The HMBC correlation between the β-hydrogens of serine and the carbonyl of L-*FOH*Orn (position 29) of lystabactin B (**2)** confirmed the serine ester (Figure S10). In addition, the fragmentation pattern in the ESIMS/MS spectrum of **2** is much more complex than **1**, which is commonly observed for cyclic peptides (Figure S11). These observations indicate that the serine side chain of lystabactin B (**2)** forms a lactone with the carbonyl of L-*FOH*Orn, resulting in a cyclic structure.

HRESIMS established the mass of the moleclular ion $[M + H]^+$ of lystabactin C (**3)** as *m/z* 858.3564, corresponding to a molecular formula of $C_{35}H_{56}N_9O_{16}$. The NMR spectra of lystabactin C (**3)** were nearly identical to **1**, with the exception of the terminal FOHOrn residue (Table S3). In lystabactin C (**3)**, the terminal FOHOrn residue is methylated resulting in a 15 mass unit increase as compared to lystabactin A (**1)**. It is uncertain whether this compound is a true natural product or an artifact of the workup.

Potentiometric Titration of Lystabactin A (1) and B (2)

A potentiometric titration was carried out to determine the protonation constants of lystabactins A (**1)** and B **(2)**. The ligand protonation constants of lystabactin A (**1**) were determined from the nonlinear refinement of the data and are given in Table 2. Similar to other catecholate siderophores, this method did not allow for the determination of the highest protonation (the meta-hydroxy of the catechol) of both compounds.[25-27] As an estimation, the first deprotonation constant of N,N-dimethyl-2,3-dihydroxybenzamide (DMB), determined previously as log K_1 = 12.1,[28] was used throughout this study. The experimentally determined protonation constants were assigned based on comparison with similar compounds. The second and third protonation constants, 9.87(7) and 9.59(5), are in the normal range for hydroxamic acids (pKa = 8-10),[29-32] and were assigned to the two hydroxamate moieties. The fourth protonation constant, 8.23(1) is assigned to the deprotonation of the primary amine in LySta. While this value is lower than expected, it is hypothesized that the multiple charged functionalities in the molecule contribute to this increased acidity. The fifth protonation constant, 6.8(1), is assigned to the *ortho*-catechol proton. By comparison, the pKa values for the three *ortho*-catechol protons of the tris-catechol siderophore, enterobactin, are 6.0, 7.5 and 8.55.[25] The increased acidity of the *ortho* group as compared to the *meta*-hydroxy group is due to conjugation of the *ortho*-hydroxy with the amide carbonyl.[33, 34] The lowest protonation constant, 3.4(1), is assigned to the carboxylic acid. The pKas determined for lystabactin B (**2)** are very similar to the values determined for lystabactin A (**1**), with the exception of the absence of the carboxylic acid (Table 3). Distribution diagrams and the potentiometric titration curves are shown in Supporting Information (Figures S17 and S18).

Table 3. Successive Protonation Constants of Lystabactins A (**1**) and B (**2**)

	1	**2**
log K_1	12.1(3)[a]	12.1(3)[a]
log K_2	9.87(7)	9.92(8)
log K_3	9.59(5)	9.66(5)
log K_4	8.23(1)	7.9(1)
log K_5	6.8(1)	6.5(2)
log K_6	3.4(1)	

[a] Estimated from DMB[28]

Iron Binding Properties of Lystabactin A (1) and B (2)

Siderophores are characterized by their high Fe(III) specificity and stability constants, enabling the producing microbe to obtain iron from a variety of environmental sources. Fe(III)-siderophore complexes often show characteristic UV-visible spectra from the ligand-to-metal charge transfer. The UV-visible spectrum of Fe(III)-**1** is shown in figure 3, displaying the characteristic ligand-to-metal charge transfer transition at 524 nm.

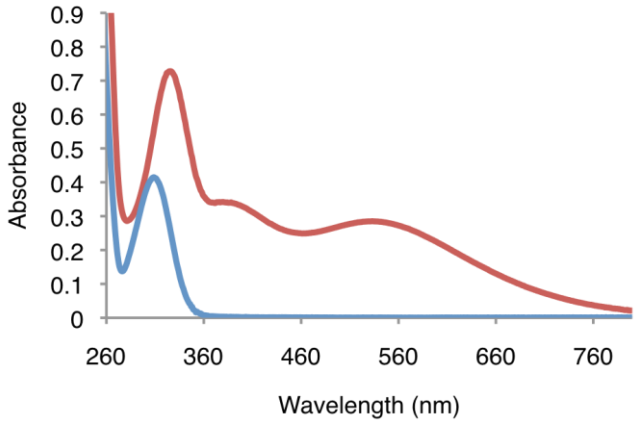

Figure 4. UV-visible spectra of apo- (blue) and Fe(III)-lystabactin A (**1**) (red). [Apo-**1**] = [Fe(III)-**1**] = 0.14 mM, in 50 mM Na-acetate buffer, pH 5.5.

The overall equilibrium reaction for the formation of FeIII-siderophore complexes is described by equation (1) and the corresponding equilibrium constant is defined by equation (2). In this definition, the siderophore is completely deprotonated, resulting in a proton independent stability constant.

$$Fe^{III}_{(aq)} + (siderophore)^{n-} = (Fe^{III}\text{-siderophore})^{3-n} \quad (1)$$

$$K = [(Fe^{III}\text{-siderophore})^{3-n}]/ [Fe^{III}_{(aq)}][(siderophore)^{n-}] \quad (2)$$

However, because siderophores have such a high affinity for ferric iron, it is difficult to directly measure the equilibrium constant of the complex formation. An approach based on the competition with EDTA, followed spectrophotometrically, allows the indirect determination of the complex stability constant.[35] At pH 5.5, it is possible to set up a measureable competition between the siderophore and EDTA for iron(III). This EDTA competition equilibrium is described by equations (3) and (4).

$$Fe^{III}\text{-siderophore} + EDTA = Fe^{III}\text{-EDTA} + siderophore \quad (3)$$

$$K_{measured} = [Fe^{III}\text{-EDTA}][siderophore]/[Fe^{III}\text{-siderophore}][EDTA] \quad (4)$$

The concentration of Fe^{III}siderophore was calculated from the absorbance at 524 nm (ε 2099 M^{-1} cm^{-1}) for lystabactin A (**1)** and 537 nm (ε 2120 M^{-1} cm^{-1}) for lystabactin B (**2) (**Figures S21 and S22). The other species in equation 2 were calculated from mass balance. To calculate the proton independent formation constant, it is necessary to correct the free ligand concentration to that of the fully deprotonated form using the appropriate α function, calculated from the protonation constants of the ligand.[31, 36, 37] Using the four required protonation constants, log values of the overall proton independent stability constants were determined to be 34.4(4) for lystabactin A (**1)** and 35.8(7) for lystabactin B (**2)**.

Because a proton independent stability constant does not give an accurate description of ferric affinity under physiological conditions, the pFe scale is often used to compare the stability of siderophores. The pFe value is the negative logarithm of the free aqueous iron(III) concentration, -log[Fe^{III}], under the defined concentrations of $[Fe^{III}]_{tot}$ = 1 μM, $[L]_{tot}$= 10 μM, and pH=7.4.[26, 38] Using these parameters, the pFe of lystabactin A (**1**) and lystabactin B (**2**) have been calculated to be 26.0 and 27.5, respectively. The pFe values for **1** and **2** are consistent with mixed bis-hydroxamate, mono-catecholate ligation, harboring increased iron(III) stability compared to the tris-hydroxamate siderophore, desferrioxamine B, due to the contribution of the catecholate group, while less stable than the tris-catecholate siderophore, enterobactin (Table 4).

Table 4. Representative Fe(III)-siderophore pFe Values.

Name	pFe
Desferrioxamine B[39]	25
1	26
2	27.5
Enterobactin[25]	34.3

In conclusion, we present the structure and iron binding properties of the lystabactins (**1**-**3**), new siderophores produced by *Pseudoalteromonas sp. S2B* isolated from the oil contaminated waters of the Gulf of Mexico after the Deepwater Horizon oil spill. The lystabactins are structurally similar to the marine siderophores alterobactins A and B and pseudoalterobactins A and B, isolated from *Alteromonas luteoviolacea* and *Pseudoalteromas sp. KP20-4* respectively.[40-42] All three sets of siderophores contain the non-proteinogenic γ-amino acid, LySta.

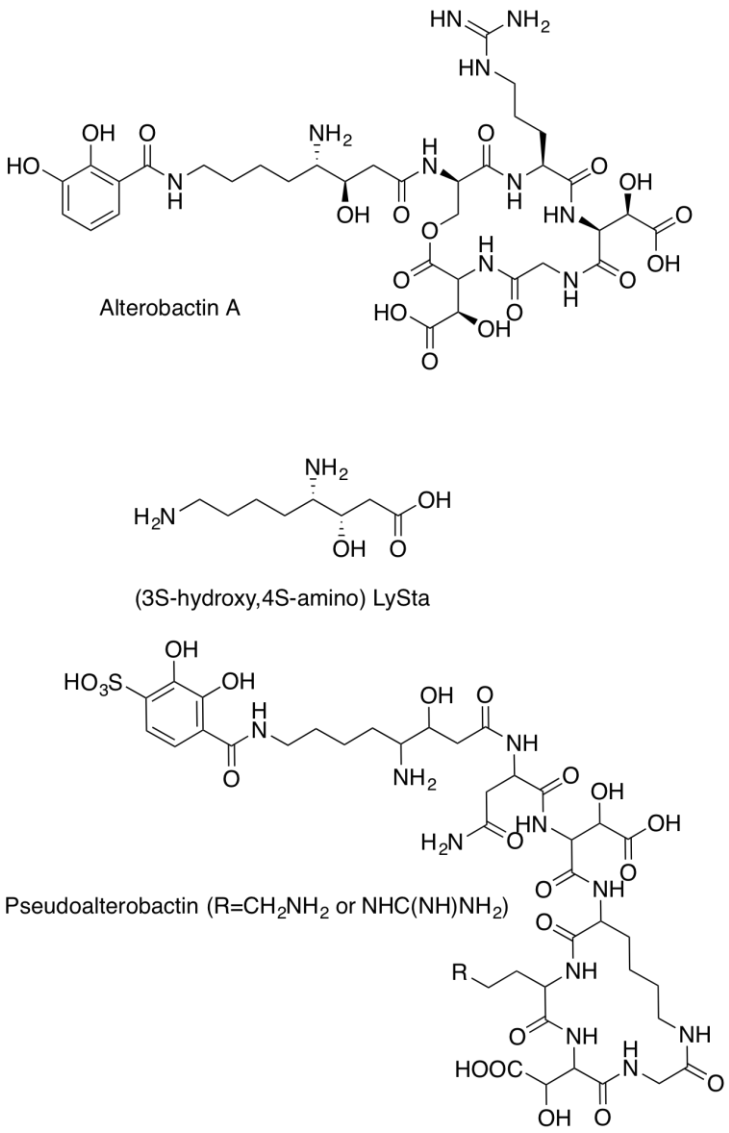

Figure 5. Other LySta containing biomolecules. Alterobactin A[40, 42] and pseudoalterobactin[41] are marine siderophores.

The configuration of the LySta moiety in the lystabactins is 3S-hydroxy, 4S-amino, while the configuration of the LySta moiety in alterobactin A and B was determined to be 3R-hydroxy, 4S-amino.[40, 42] The configuration of LySta in pseudoalterobactin A and B was not determined.[41] The (3S-hydroxy, 4S-amino)-LySta isomer has been chemically synthesized and incorporated into a tetrapeptide and shown to act as an aspartic protease inhibitor.[43] To our knowledge, the

lystabactins are the first examples of natural products containing (3S,4S)-LySta. The inclusion of non-proteinogenic amino acids into these siderophores suggests a nonribosomal origin of biosynthesis and studies detailing the biosynthesis of **1** and **2** are now underway.

Experimental Section

General Experimental Procedures. A Varian Cary-Bio 300 UV-visible spectrophotometer was used for ultraviolet and visible spectrophotometry. 1D (^{1}H and ^{13}C), and 2D (^{1}H-^{1}H gCOSY, ^{1}H-^{1}H TOCSY, ^{1}H-^{13}C HSQC, and ^{1}H-^{13}C HMQC) NMR spectra were obtained using a Bruker Avance II 800 Ultrashield Plus and Varian Unity Inova AS600 spectrometers in methanol-d_4 and dimethyl sulfoxide-d_6 (Cambridge Isotope Laboratories). Molecular masses and partial connectivity of **1-3** were determined by electrospray ionization mass spectrometry (ESIMS) and tandem mass spectrometry (ESIMS/MS), with argon as a collision gas, using a Micromass QTOF-2 mass spectrometer (Waters Corp.). A Varian Cary-Bio 300 UV-visible spectrophotometer was used for ultraviolet and visible spectrophotometry.

Bacterial Isolation. *Pseudoalteromonas sp.* S2B was isolated from the surface of an open ocean water sample collected from the oil contaminated waters of the Gulf of Mexico after the BP oil spill in 2010.

Phylogenetic Analysis. Genomic DNA was isolated using the chloroform:phenol:isoamyl alcohol extraction procedure from cells grown in 5 mL marine broth cultures.[44] The 16S rRNA genes were PCR amplified in 50 μl reaction mixures with the universal primers 27F and 1492R.[45] Cycling conditions were as follows: initial denaturation at 90 °C for 3 min, 35 cycles of 94 °C for 30 s, 55 °C for 1 min, and 72 °C for 100 s, and a final extension of 10 min at 72 °C. PCR products were visualized on a 1% (wt/vol) agarose gel stained with ethidium bromide,

revealing the presence of only one band at 1500 bp. PCR products were cloned with a TOPO TA cloning kit according to the manufacturer's instructions (Invitrogen). Plasmids were purified using PureLink Quick Plasmid Miniprep Kit (Invitrogen) and checked for inserts by digestion with Eco R1 restriction endonuclease. Samples were sequenced using M13 forward and reverse primers (UC Berkeley DNA Sequencing Facility). The sequence (Genbank accession number KC_517483) was compared to those in databases using the Basic Local Alignment Tool (BLAST) algorithm to identify sequences with a high degree of similarity.

Growth on Crude Oil. *Pseudoalteromonas sp.* S2B was grown in a modified synthetic seawater medium[15] containing (per liter of doubly distilled water (Barnstead Nanopure II)), 23 g NaCl, 0.75 g KCl, 1 g NH_4Cl, 6.16 g $MgSO_4 \bullet 7H2O$, 5.08 $MgCl_2 \bullet 6H_2O$ g and 1.5 g $CaCl_2$ (pH 7.8) autoclaved at 120 °C for 20 min. Sterile solutions of $FeSO_4$, PO_4 (final concentration 0.2 and 2 mmol l^{-1}, respectively) and crude oil (1g l^{-1}) from Platform Gail, a well offshore Santa Barbara, (1g l^{-1}) were added before inoculation. Bacterial growth was monitored through measurement of the optical density of the culture (600 nm) using a Varian Cary-Bio 300 UV-visible spectrophotometer (Figure S1).

Siderophore Isolation. *Pseudoalteromonas sp*. S2B was cultured in low-iron artificial seawater medium (2 L) containing casamino acids (10 g/L), NH_4Cl (19 mM), sodium glycerophosphate hydrate (4.6 mM), $MgSO_4$ (50 mM), $CaCl_2$(10 mM), trace metal grade NaCl (0.3 M), KCl (10 mM), glycerol (41 mM), HEPES buffer (10 mM; pH 7.4), $NaHCO_3$ (2 mM), biotin (8.2 μM), niacin (1.6 μM), thiamin (0.33 μM), 4-aminobenzoic acid (1.46 μM), panthothenic acid (0.21 μM), pyridoxine hydrochloride (5 μM), cyanocobalamin (0.07 μM), riboflavin (0.5 μM), and folic acid (0.5 μM) in acid-washed Erlenmeyer flasks (4 L). Two-liter cultures were grown on an orbital shaker (180 rpm) at room temperature for approximately 24 h

until the liquid chrome azurol sulfonate (CAS) test indicated the presence of iron(III)-binding compounds in the culture medium. Cultures were harvested by centrifugation (6000 rpm, 30 min), and Amberlite XAD-2 resin (Supelco) was added to the decanted supernatant (ca. 100 g/L), and the resulting mixture was shaken (4 h at 120 rpm). The filtered XAD resin was washed with doubly deionized H_2O (2 L; Barnstead Nanopure II), and the siderophores were eluted with MeOH/H_2O (1:1). The fractions containing siderophores were identified by the CAS assay and concentrated under vacuum. The siderophores were purified by reversed-phase HPLC on a preparative C_4 column (22 mm internal diameter, i.d., × 250 mm length, Vydac) with a gradient from H_2O (doubly deionized with 0.05% trifluoro acetic acid (TFA)) to 50% MeOH (with TFA; 0.05%) over 40 min. The eluent was continuously monitored (215 nm). Fractions were manually collected and immediately concentrated under vacuum. Samples were ultrapurified chromatographically by preparative C_4 (22 mm i.d. × 250 mm L, Vydac) using the same program as described above. Purified samples were lyophilized and stored at −80 °C.

Siderophores eluted at 28.2 min (**1**), 31.1 min (**2**), and 32 min (**3**). Approximately 4 mg, 6 mg, and 3 mg of siderophores (**1**−**3**, respectively) were isolated per 2 L of culture.

Lystabactin A (1): colorless oil, UV (50 mM Na-acetate buffer, pH=5.5) λ_{max} (log ε) 309 (3.41) nm; ^{1}H, ^{13}C, and 2D NMR data, Table 1; HRESIMS *m/z* 866.3484 $[M+Na]^+$ (calcd for $C_{34}H_{53}N_9O_{16}Na$, 866.3508).

Lystabactin B (2): colorless oil, UV (50 mM Na-acetate buffer, pH=5.5) λ_{max} (log ε) 310 (3.45) nm; ^{1}H, ^{13}C, and 2D NMR data, Table S1; HRESIMS *m/z* 826.3564 $[M+H]^+$ (calcd for $C_{34}H_{52}N_9O_{15}$, 826.3583).

Lystabactin C (3): yellow oil, UV (50 mM Na-acetate buffer, pH=5.5) λ_{max} (log ε) 309 (3.41) nm; ^{1}H, ^{13}C, and 2D NMR data, Table S2; HRESIMS *m/z* 858.3564 $[M+H]^+$ (calcd for $C_{35}H_{56}N_9O_{16}$, 858.3767).

Marfey's Amino Acid Analysis. Five hundred micrograms of **1**, **2** and **3** were dissolved in 200 μL of 55% HI and heated at 110 °C for 24 h. The solutions were evaporated to dryness and re-dissolved in 100 μL of H_2O. 40 μL of 1M $NaHCO_3$ and 200 μL of a 1% solution of Marfey's reagent[18] ((*N*$^{\alpha}$-(2,4-dinitro-5-fluorophenyl)-L-alaninamide (FDAA)) in acetone was added and the solution was heated for 1 h at 40 °C. The reaction was quenched with 20 μL of HCl. The derivatized samples were analyzed by HPLC on an analytical YMC ODS-AQ C18 column (4.6 mm, i.d. x 250 mm L, Waters Corp.) using a linear gradient from 90% doubly deionized H_2O(with 0.05% TFA)/10% CH_3CN to 60% ddH_2O (with 0.05% TFA)/ 40% CH_3CN over 45 min and the eluent was monitored at 340 nm. Stereochemical assignments were made by comparison with the retention times of Marfey's derivatives prepared from authentic amino acid standards of D/L-serine, D/L-ornithine, and D/L-aspartic acid (Sigma-Aldrich) using the method described above. (3S,4S)-LySta and (3R,4S)-LySta were synthesized according to the method of Maibaum et al.[21] Retention times (min) of the FDAA amino acid derivatives used as standards were L-serine (22.0 min), D-serine (24.6 min), L-aspartic acid (26.4 min), D-aspartic acid (28.4 min), L-ornithine (mono α–derivative (22.9 min), mono ε–derivative (23.7 min), bis-derivative (46.0 min)), D-ornithine (mono α–derivative (18.0 min), mono ε–derivative (23.7 min), bis-derivative (42.0 min)), (3R-hydroxy, 4S-amino)-Lysta (mono γ-derivative (20.7 min), mono C8-derivative (25.4 min), bis-derivative (44.6 min)), (3S-hydroxy, 4S-amino)-Lysta (mono γ-derivative (22.5 min), mono C8-derivative (25.4 min), bis-derivative (45.8 min)). FDAA-derivatized hydrolysis products of **1** were (3S-hydroxy, 4S-amino)-Lysta (mono γ-derivative

(22.5 min), mono C8-derivative (25.4 min), bis-derivative (45.8 min)), L-ornithine (mono α–derivative (23.0 min), mono ε–derivative (23.8 min), bis-derivative (46.1 min)), D-serine (24.5 min), and D-aspartic acid (28.2 min). FDAA-derivatized hydrolysis products of **2** were (3S-hydroxy, 4S-amino)-Lysta (mono γ-derivative (22.3 min), mono C8-derivative (25.1 min), bis-derivative (45.5 min)), L-ornithine (mono α–derivative (22.8 min), mono ε–derivative (23.4 min), bis-derivative (46.0 min)), D-serine (24.2 min), and D-aspartic acid (27.9 min).FDAA-derivatized hydrolysis products of **3** were (3S-hydroxy, 4S-amino)-Lysta (mono γ-derivative (22.4 min), mono C8-derivative (25.2 min), bis-derivative (45.5 min)), L-ornithine (mono α–derivative (22.9 min), mono ε–derivative (23.6 min), bis-derivative (46.1 min)), D-serine (24.4 min), and D-aspartic acid (28.1 min).

Potentiometric Titration. Potentiometric titrations were performed using a Radiometer PHM240 pH meter with a pHC4406 combination electrode. The electrode was calibrated by the classical method, titration of a 0.10 M HCl (standardized with recrystallized borax to a methyl red endpoint) with 0.10 M NaOH (standardized with potassium hydrogen phthalate (Aldrich, primary standard grade) to a phenolphthalein end point). The computer program GLEE was used to calibrate the glass electrode and to calculate the carbonate percentage in the NaOH solution used.[35, 46, 47] Titrations were carried out in jacketed three necked titration vessels connected to a constant temperature water bath and held at 25.0(1) °C. Samples were degassed with Ascarite-scrubbed argon and kept under a positive pressure of argon throughout the titration. Standardized NaOH (0.1 M) was added to a solution of approximately 130 μM **1** or **2** in 0.1 M NaCl background electrolyte using a Gilmont microburet. Ligand protonation constants were determined from the nonlinear refinement of the potentiometric titration data using the program Hyperquad.[48]

Stability Constant Determination. A spectrophotometric competition with EDTA was used to determine the stability constants of Fe(III)-**1** and Fe(III)-**2**. Solutions for the EDTA competition were prepared in a 50 mM acetate (pH 5.5) buffer containing 0.1 M NaCl, and were allowed to equilibrate for 24 h at 25 °C. Typical solutions were 100 μM Fe(III) and ligand concentration with variable EDTA concentrations ([EDTA] = 20 μM, 40 μM, 80 μM, 100 μM and 200 μM). The equilibrium being monitored in this reaction is shown in Eq. 3-4. An example of the spectra measured in the competition reaction is shown in Figure S19.

$K_{measured}$ was calculated using the concentration of [Fe(III)-**1**] or [Fe(III)-**2**] determined spectrophotometrically; λ_{max} 524 nm, ε 2099 M^{-1} cm^{-1} and λ_{max} 537 nm, ε 2120 M^{-1} cm^{-1}, respectively. Reported stability constants are the average of three separate trials.

Acknowledgment. Funding from CHE-1059067 (A.B.) is gratefully acknowledged. We thank J. Pavlovich (MS), H. Zhou (NMR) at UCSB, and Professor D. Valentine at UCSB.

Supporting Information Available. The growth curve of *Pseudoalteromonas sp. S2B* in SSW + 0.1% cruide oil, ^{1}H NMR and ^{13}C NMR spectra of **1**-**3**, and ^{1}H-^{13}C HSQC and ^{1}H-^{13}C HMBC Spectra of **1**-**3**, tabulated NMR data for **2** and **3** ESIMS/MS spectra of **2** and **3**.

References:

1. Johnson, K. S.; Gordon, R. M.; Coale, K. H., What controls dissolved iron concentrations in the world ocean? . *Mar. Chem.* **1997,** 57, 181-186.

2. Bruland, K. W.; Donat, J. R.; Hutchins, D. A., Interactive influences of bioactive trace metals on biological production in oceanic waters. *Limnol. Oceanogr.* **1991,** 36, 1555-77.

3. Chavez, F. P.; Buck, K. R.; Coale, K. H.; Martin, J. H.; DiTullio, G. R.; Welschmeyer, N. A.; Jacobson, A. C.; Barber, R. T., Growth rates, grazing, sinking, and iron limitation of equatorial Pacific phytoplankton. *Limnol. Oceanogr.* **1991,** 36, 1816-33.

4. Wu, J.; Luther, G. W., III, Size-fractionated iron concentrations in the water column of the western North Atlantic Ocean. *Limnol. Oceanogr.* **1994,** 39, 1119-29.

5. Wu, J.; Luther III, G. W., Spatial and temporal distribution of iron in the surface water of the northwestern Atlantic Ocean. *Geochim. Cosmochim. Acta* **1996,** 60, 2729-2741.

6. Crosa, J. H.; Mey, A. R.; Payne, S. M.; Editors, *Iron Transport in Bacteria*. American Society for Microbiology: 2004; p 499 pp.

7. Boukhalfa, H.; Crumbliss, A. L., Chemical aspects of siderophore mediated iron transport. *BioMetals* **2002,** 15, 325-339.

8. Prince, R. C.; Varadaraj, R.; Fiocco, R. J.; Lessard, R. R., Bioremediation as an oil spill response tool. *Environ. Technol.* **1999,** 20, 891-896.

9. Leahy, J. G.; Colwell, R. R., Microbial degradation of hydrocarbons in the environment. *Microbiol. Rev.* **1990,** 54, 305-15.

10. Bragg, J. R.; Prince, R. C.; Harner, E. J.; Atlas, R. M., Effectiveness of bioremediation for the Exxon Valdez oil spill. *Nature* **1994,** 368, 413-18.

11. Swannell, R. P. J.; Croft, B. C.; Grant, A. L.; Lee, K., Evaluation of bioremediation agents in beach microcosms. *Spill Science & Technology Bulletin* **1995,** 2, 151-159.

12. Bosello, M.; Robbel, L.; Linne, U.; Xie, X.; Marahiel, M. A., Biosynthesis of the Siderophore Rhodochelin Requires the Coordinated Expression of Three Independent Gene Clusters in *Rhodococcus jostii* RHA1. *J. Am. Chem. Soc.* **2011,** 133, 4587-4595.

13. Kreutzer, M. F.; Kage, H.; Nett, M., Structure and Biosynthetic Assembly of Cupriachelin, a Photoreactive Siderophore from the Bioplastic Producer *Cupriavidus necator* H16. *J. Am. Chem. Soc.* **2012,** 134, 5415-5422.

14. Dibble, J. T.; Bartha, R., Effect of iron on the biodegradation of petroleum in seawater. *Appl. Environ. Microbiol.* **1976,** 31, 544-50.

15. Husain, S., Effect of Ferric Iron on Siderophore Production and Pyrene Degradation by Pseudomonas fluorescens 29L. *Curr. Microbiol.* **2008,** 57, 331-334.

16. Bergeron, R. J.; Huang, G.; Smith, R. E.; Bharti, N.; McManis, J. S.; Butler, A., Total synthesis and structure revision of petrobactin. *Tetrahedron* **2003,** 59, 2007-2014.

17. Hickford, S. J. H.; Küpper, F. C.; Zhang, G.; Carrano, C. J.; Blunt, J. W.; Butler, A., Petrobactin Sulfonate, a New Siderophore Produced by the Marine Bacterium Marinobacter hydrocarbonoclasticus. *J. Nat. Prod.* **2004,** 67, 1897-1899.

18. Gauglitz, J. M.; Zhou, H.; Butler, A., A suite of citrate-derived siderophores from a marine Vibrio species isolated following the Deepwater Horizon oil spill. *J. Inorg. Biochem.* **2012,** 107, 90-95.

19. Tapilatu, Y.; Acquaviva, M.; Guigue, C.; Miralles, G.; Bertrand, J. C.; Cuny, P., Isolation of alkane-degrading bacteria from deep-sea Mediterranean sediments. *Lett. Appl. Microbiol.* **2010,** 50, 234-236.

20. Schwyn, B.; Neilands, J. B., Universal chemical assay for the detection and determination of siderophores. *Anal. Biochem.* **1987,** 160, 47-56.

21. Maibaum, J.; Rich, D. H., A facile synthesis of statine and analogs by reduction of .beta.-keto esters derived from Boc-protected amino acids. HPLC analyses of their enantiomeric purity. *J. Org. Chem.* **1988,** 53, 869-873.

22. Briskot, G.; Taraz, K.; Budzikiewicz, H., Bacterial Constituents, XXXVII. Pyoverdin-Type Siderophores from *Pseudomonas aeruginosa*. *Liebigs Ann. Chem.* **1989,** 1989, 375-384.

23. Marfey, P.; Ottesen, M., Determination of D-amino acids. I. Hydrolysis of DNP-L-amino acid methyl esters with carboxypeptidase-Y. *Carlsberg Res. Commun.* **1984,** 49, 585-90.

24. Stephan, H.; Freund, S.; Meyer, J.-M.; Winkelmann, G.; Jung, G., Structure Elucidation of the Gallium–Ornibactin Complex by 2D-NMR Spectroscopy. *Liebigs Ann. Chem.* **1993,** 1993, 43-48.

25. Loomis, L. D.; Raymond, K. N., Solution equilibria of enterobactin and metal-enterobactin complexes. *Inorg. Chem.* **1991,** 30, 906-911.

26. Abergel, R. J.; Zawadzka, A. M.; Raymond, K. N., Petrobactin-Mediated Iron Transport in Pathogenic Bacteria: Coordination Chemistry of an Unusual 3,4-Catecholate/Citrate Siderophore1. *J. Am. Chem. Soc.* **2008,** 130, 2124-2125.

27. Tomišić, V.; Blanc, S.; Elhabiri, M.; Expert, D.; Albrecht-Gary, A.-M., Iron(III) Uptake and Release by Chrysobactin, a Siderophore of the Phytophatogenic Bacterium *Erwinia chrysanthemi*. *Inorg. Chem.* **2008,** 47, 9419-9430.

28. Harris, W. R.; Carrano, C. J.; Cooper, S. R.; Sofen, S. R.; Avdeef, A. E.; McArdle, J. V.; Raymond, K. N., Coordination chemistry of microbial iron transport compounds. 19. Stability

constants and electrochemical behavior of ferric enterobactin and model complexes. *J. Am. Chem. Soc.* **1979,** 101, 6097-6104.

29. Monzyk, B.; Crumbliss, A. L., Acid dissociation constants (Ka) and their temperature dependencies (ΔH_a, ΔS_a) for a series of carbon- and nitrogen-substituted hydroxamic acids in aqueous solution. *J. Org. Chem.* **1980,** 45, 4670-4675.

30. Brink, C. P.; Fish, L. L.; Crumbliss, A. L., Temperature-dependent acid dissociation constants (K_a, ΔH_a, ΔS_a) for some C-aryl hydroxamic acids: the influence of carbon and nitrogen substituents on hydroxamate anion solvation in aqueous solution. *J. Org. Chem.* **1985,** 50, 2277-2281.

31. Dhungana, S.; Harrington, J. M.; Gebhardt, P.; Möllmann, U.; Crumbliss, A. L., Iron Chelation Equilibria, Redox, and Siderophore Activity of a Saccharide Platform Ferrichrome Analogue. *Inorg. Chem.* **2007,** 46, 8362-8371.

32. Carrano, C. J.; Cooper, S. R.; Raymond, K. N., Coordination chemistry of microbial iron transport compounds. 11. Solution equilibriums and electrochemistry of ferric rhodotorulate complexes. *J. Am. Chem. Soc.* **1979,** 101, 599-604.

33. Llinas, M.; Wilson, D. M.; Neilands, J. B., Effect of metal binding on the conformation of enterobactin. Proton and carbon-13 nuclear magnetic resonance study. *Biochemistry* **1973,** 12, 3836-3843.

34. Mies, K. A.; Gebhardt, P.; Möllmann, U.; Crumbliss, A. L., Synthesis, siderophore activity and iron(III) chelation chemistry of a novel mono-hydroxamate, bis-catecholate siderophore mimic: NŒ±,-NŒµ-Bis[2,3-dihydroxybenzoyl]-l-lysyl-(Œ≥-N-methyl-N-hydroxyamido)-l-glutamic acid. *J. Inorg. Biochem.* **2008,** 102, 850-861.

35. Martell, A. E.; Smith, R.M., *Critical stability constants*. Plenum Press: New York:, 1974, pp 415.

36. Hou, Z.; Raymond, K. N.; O'Sulliva, B.; Esker, T. W.; Nishio, T., A Preorganized Siderophore:,Äâ Thermodynamic and Structural Characterization of Alcaligin and Bisucaberin, Microbial Macrocyclic Dihydroxamate Chelating Agents1. *Inorg. Chem.* **1998,** 37, 6630-6637.

37. Zhang, G.; Amin, S. A.; Kupper, F. C.; Holt, P. D.; Carrano, C. J.; Butler, A., Ferric Stability Constants of Representative Marine Siderophores: Marinobactins, Aquachelins, and Petrobactin. *Inorg. Chem.* **2009,** 48, 11466-11473.

38. Harris, W. R.; Carrano, C. J.; Raymond, K. N., Spectrophotometric determination of the proton-dependent stability constant of ferric enterobactin. *J. Am. Chem. Soc.* **1979,** 101, 2213-2214.

39. Evers, A.; Hancock, R. D.; Martell, A. E.; Motekaitis, R. J., Metal ion recognition in ligands with negatively charged oxygen donor groups. Complexation of iron(III), gallium(III), indium(III), aluminum(III), and other highly charged metal ions. *Inorg. Chem.* **1989,** 28, 2189-2195.

40. Holt, P. D.; Reid, R. R.; Lewis, B. L.; Luther, G. W.; Butler, A., Iron(III) Coordination Chemistry of Alterobactin A: A Siderophore from the Marine Bacterium Alteromonas luteoviolacea. *Inorg. Chem.* **2005,** 44, 7671-7677.

41. Kanoh, K.; Kamino, K.; Leleo, G.; Adachi, K.; Shizuri, Y., Pseudoalterobactin A and B, New Siderophores Excreted by Marine Bacterium Pseudoalteromonas sp. KP20-4. *J. Antibiotic.,* **2003**, 56, 871-875.

42. Reid, R. T.; Live, D. H.; Faulkner, D. J.; Butler, A., A siderophore from a marine bacterium with an exceptional ferric ion affinity constant. *Nature* **1993,** 366, 455-458.

43. Salituro, F. G.; Agarwal, N.; Hofmann, T.; Rich, D. H., Inhibition of aspartic proteinases by peptides containing lysine and ornithine side-chain analogs of statine. *J. Med. Chem.* **1987,** 30, 286-295.

44. Wilson, K., Preparation of Genomic DNA from Bacteria. In *Current Protocols in Molecular Biology*, John Wiley & Sons, Inc.: 2001.

45. Vraspir, J.; Holt, P.; Butler, A., Identification of new members within suites of amphiphilic marine siderophores. *BioMetals* **2011,** 24, 85-92.

46. Gans, P.; O'Sullivan, B., GLEE, a new computer program for glass electrode calibration. *Talanta* **2000,** 51, 33-37.

47. Harrington, J. M.; Chittamuru, S.; Dhungana, S.; Jacobs, H. K.; Gopalan, A. S.; Crumbliss, A. L., Synthesis and Iron Sequestration Equilibria of Novel Exocyclic 3-Hydroxy-2-pyridinone Donor Group Siderophore Mimics. *Inorg. Chem.* **2010,** 49, 8208-8221.

48. Gans, P.; Sabatini, A.; Vacca, A., Investigation of equilibria in solution. Determination of equilibrium constants with the HYPERQUAD suite of programs. *Talanta* **1996,** 43, 1739-1753.

TOC Synopsis: